F. W. Brust

S. Rahman

N. D. Ghadiali

Battelle Columbus Laboratories,
Columbus, OH 43201-2693

Elastic-Plastic Analysis of Small Cracks in Tubes

Introduction

Analytical methods for predicting the elastic or elastic-plastic behavior of large circumferential through-wall cracks in tubes subjected to bending, tension, or combined bending and tension are well developed. Gilles and Brust (1991) and Gilles et al. (1991) summarize five such methods and provide a number of comparisons between analytically predicted results and experimental data. These techniques consist of developing a method for estimating the value of the J-integral. Classical J-tearing theory is utilized for the analyses. A method has also been recently developed to estimate J for a through-wall crack in a pipe weld (Rahman et al., 1991; Rahman and Brust, 1992).

Unfortunately, the ability of these J-estimation techniques to predict the crack growth behavior for small cracks (≤ 12 percent of the circumference) has not been established, even though such small cracks are often the concern in practical structures.[1] Indeed, the finite element solutions compiled in the GE/EPRI handbook (Kumar et al., 1984) appear quite inadequate for small-size cracks (Gilles and Brust, 1991; Gilles et al., 1991). This paper presents the results of a series of finite element solutions for small cracks tabulated in the spirit of the handbook (Kumar et al., 1984). Specifically, the solutions of Kumar et al. (1984) for $\theta/\pi = 1/8$, $1/16$ are redone for Ramberg-Osgood coefficients $n = 1$, 3, 5, 7, 10 for bending, where θ is the half-crack angle.

The theoretical background for the development and use of simplified elastic-plastic fracture methods is fully discussed in Gilles and Brust (1991). Here we provide the solutions for J-integral and the crack opening displacements for small crack problems under pure bending. Ongoing work will complete these solutions for tension and for combined tension-bending loads.

The GE/EPRI Estimation Scheme

The GE/EPRI method takes advantage of the scaling properties in linear and nonlinear elasticity to interpolate over the range from small-scale yielding to large-scale yielding and to normalize fracture parameters, such as J, crack opening displacement (COD), and displacements. The elastic-plastic solution is obtained by superposition of a small-scale yielding solution and of the fully plastic solution. The stress-strain law is defined by a Ramberg-Osgood relation

$$\frac{\epsilon}{\epsilon_o} = \frac{\sigma}{\sigma_o} + \alpha\left(\frac{\sigma}{\sigma_o}\right)^n \tag{1}$$

where σ_o is an arbitrary reference stress usually defined as the yield stress, α and n are curve-fitting parameters, and $\epsilon_o = \sigma_o/E$.

This normalization reduces the fracture parameter determination to the computation of coefficients depending, for given types of geometry and loading, only on the strain-hardening coefficient n and a few geometrical parameters. Tabulated values of these coefficients were computed (Kumar et al., 1984, 1981) using the finite element technique. J for a through-wall cracked pipe in bending is written in the following form:

$$J = J_e + J_p = f_1\frac{M^2}{E} + \alpha\sigma_o\epsilon_o a\left(1 - \frac{\theta}{\pi}\right)h_1\left(\frac{M}{M_o}\right)^{n+1} \tag{2a}$$

In Eq. (2), θ is the half-crack angle, a is the half-crack length ($a = R\theta$), R is the mean radius of pipe, and M_o is the limit moment, defined in Kumar et al. (1984) (see Fig. 1). Also,

$$f_1 = f_1\left(a_e, \frac{R}{t}\right) \tag{2b}$$

$$h_1 = h_1\left(\frac{\theta}{\pi}, \frac{R}{t}, n\right) \tag{2c}$$

and are tabulated (where t is the pipe wall thickness). In the pipe bending case, M = the moment and the effective crack size, a_e, based on an Irwin plastic zone correction, is written as

$$a_e = a + \frac{r_y}{1 + \left(\frac{M}{M_o}\right)^2} \tag{3a}$$

$$a = R\theta \tag{3b}$$

[1] These methods have been validated for large cracks; e.g., see Brust (1987) and Gilles and Brust (1991).

Contributed by the OMAE Division and presented at the 11th International Symposium and Exhibit on Offshore Mechanics and Arctic Engineering, Calgary, Alberta, Canada, June 7-12, 1992, of THE AMERICAN SOCIETY OF MECHANICAL ENGINEERS. Manuscript received by the OMAE Division, 1992; revised manuscript received June 20, 1994. Associate Technical Editor: H. Chong Rhee.

Table 1 Matrix of finite element calculations (total of 30 analyses for bending)

Model no.	Model name	R/t	$n^{(a)}$	θ/π	Remarks	Loading
1	CASE1A3DM	5	1,3,5,7,10	0.0625	5 Runs	Bending
2	CASE2A3DM	10	1,3,5,7,10	0.0625	5 Runs	Bending
3	CASE3A3DM	20	1,3,5,7,10	0.0625	5 Runs	Bending
4	CASE1B3DM	5	1,3,5,7,10	0.1250	5 Runs	Bending
5	CASE2B3DM	10	1,3,5,7,10	0.1250	5 Runs	Bending
6	CASE3B3DM	20	1,3,5,7,10	0.1250	5 Runs	Bending

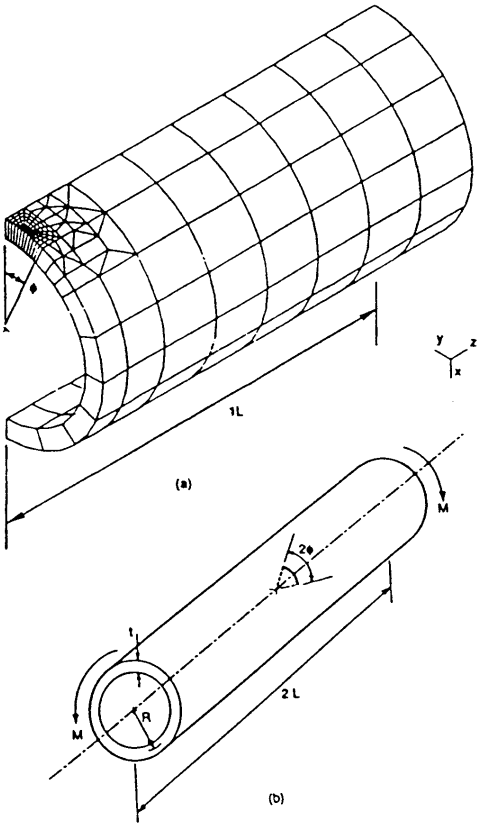

Fig. 1 Typical finite element mesh used for analysis (1/4 model) and (b) circumferential cracked pipe geometry

$$r_y = \frac{1}{2\pi}\left[\frac{n-1}{n+1}\right]\left(\frac{K}{\sigma_o}\right)^2 \tag{3c}$$

where K, the stress intensity factor, is a function of a and not of a_e. Other parameters such as crack opening displacement and load-point rotations were also evaluated in Kumar et al. (1984).

The GE/EPRI method, as developed for TWC pipe, appears to be too conservative, i.e., the compiled values of h_1, and, hence, J, are too large. In fact, for the smaller crack sizes, the results appear quite inadequate. Indeed, the pipe rotations due to the crack are negative for $\theta/\pi = 1/16$, as compiled in Kumar et al. (1984) for both elastic and plastic solutions. As discussed in Gilles and Brust (1991), Gilles et al. (1991), Brust and Gilles (1992), and Brust (1987), this problem may be due to the use of the 9-node shell element in Kumar et al. (1984) to produce the solutions, and overly stiff results occurred. Here we recompute the solutions of Kumar et al. (1984) for $\theta/\pi = 1/8$ and $\theta/\pi = 1/16$. In this fashion, more reliable predictions of crack instability for the smaller crack sizes using the GE/EPRI scheme are expected.

Finite Element Model and Analysis Matrix

Six finite element meshes have been developed, one for each case listed in Table 1. A typical finite element mesh and geometric definitions are illustrated in Fig. 1. A quarter model is used by taking advantage of symmetry. Twenty-node isoparametric brick elements are being used with focused elements at the crack tip. Only one element through the pipe wall is used, and, as such, the tabulated results should be considered as average values through the pipe wall. Results for tension loading and combined tension and bending are currently being compiled.

The elastic solutions are developed using elastic properties. A deformation theory plasticity algorithm in the ABAQUS finite element code is used to generate the plastic solution. Because a through-wall cracked pipe subjected to bending is a plane stress problem, the special (hybrid) elements in the ABAQUS library which adequately handle plastic incompressibility are not necessary. A reduced (2 × 2) Gauss quadrature integration rule is utilized.

The GE/EPRI handbook (Kumar et al., 1984) compiled tables whereby J, the crack mouth opening displacement (at the center of the crack), δ, are tabulated for specific geometric and material parameters. The parameters include R/t, θ, and the Ramberg-Osgood power law exponent, n. For a uniaxial tensile bar, the Ramberg-Osgood relation is as written in Eq. (1).

Here we follow the convention of Kumar et al. (1984) and compile, for J (see Eq. 2(a)), the crack opening displacement (δ) and the additional pipe rotation due to the presence of the crack (ϕ^c)

$$\delta = \delta_e + \delta_p = f_2\frac{M}{E} + \alpha\epsilon_o a h_2\left(\frac{M}{M_o}\right)^n \tag{4a}$$

$$\phi_T^c = \phi_e^c + \phi_p^c$$

$$\phi_T^c = f_4\frac{M}{\epsilon} + \alpha\epsilon_o h_4\left(\frac{M}{M_o}\right)^n \tag{4b}$$

where δ_e and δ_p are elastic and plastic contributions, respectively.

For the elastic contribution, using the GE/EPRI convention (Eq. (2)), we write

$$f_1\left(\frac{\theta}{\pi}, \frac{R}{t}\right) = \pi a\left(\frac{R}{t}\right)^2 F^2\left(\frac{\theta}{\pi}, \frac{R}{t}\right) \tag{5}$$

$$f_2\left(\frac{\theta}{\pi}, \frac{R}{t}\right) = 4a\frac{R}{t} V_1\left(\frac{\theta}{\pi}, \frac{R}{t}\right) \tag{6}$$

$$f_4\left(\frac{\theta}{\pi}, \frac{R}{t}\right) = 4\frac{R}{t} V_3\left(\frac{\theta}{\pi}, \frac{R}{t}\right) \tag{7}$$

Table 2 Check case—$R/t = 10$, $\theta/\pi = 1/2$, $n = 3$

J-integral value	GE/EPRI	3-D-solid ABAQUS
h_1	2.105	2.105
h_2	3.331	3.195
h_4	3.232	4.635

Table 3 F, V_1, for bending ($R/t = 5$, 10, 20) (ABAQUS 3-D-solid solution) this represents the $n = 1$ case of Table 1

		$R/t = 5$	$R/t = 10$	$R/t = 20$
$\theta/\pi = 1/16$	F	1.022	1.049	1.097
	V_1	1.234	1.206	1.111
	V_3	0.028	0.035	0.098
$\theta/\pi = 1/8$	F	1.103	1.208	1.418
	V_1	1.388	1.480	1.482
	V_3	0.126	0.160	0.231

Table 4 h-functions for through-cracks in bending ($R/t = 5$) (ABAQUS—3-D solid solution)

		$n = 3$	$n = 5$	$n = 7$	$n = 10$
$\theta/\pi = 1/16$	h_1	5.451	5.766	5.681	5.263
	h_2	6.896	7.003	6.715	6.087
	h_4	0.826	1.452	1.879	2.371
$\theta/\pi = 1/8$	h_1	4.484	3.976	3.372	2.464
	h_2	5.820	4.999	4.164	2.959
	h_4	1.194	1.454	1.461	1.291

Table 5 h-functions for through-cracks in bending ($R/t = 10$) (ABAQUS—3-D solid solution)

		$n = 3$	$n = 5$	$n = 7$	$n = 10$
$\theta/\pi = 1/16$	h_1	6.225	6.761	6.784	6.749
	h_2	7.422	7.739	7.632	7.527
	h_4	1.156	1.802	2.220	2.826
$\theta/\pi = 1/8$	h_1	5.791	5.512	4.790	3.823
	h_2	6.693	6.319	5.329	4.221
	h_4	1.550	1.886	1.864	1.713

Table 6 h-functions for through-cracks in bending ($R/t = 20$) (ABAQUS—3-D solid solution)

		$n = 3$	$n = 5$	$n = 7$	$n = 10$
$\theta/\pi = 1/16$	h_1	7.044	8.022	8.756	8.815
	h_2	7.073	8.050	8.787	8.812
	h_4	1.505	2.348	3.087	3.770
$\theta/\pi = 1/8$	h_1	8.448	8.281	7.748	6.524
	h_2	7.498	7.491	7.160	5.890
	h_4	2.216	2.738	2.963	2.728

In Eqs. (5) to (7), I is the moment of inertia of the uncracked section, which for large R/t is written as

$$I = \pi R^3 t$$

and F, V_1, and V_3, are compiled from the finite element solutions. Note that F is the function conventionally defined in the stress intensity factor definition as

$$K_I = \sigma\sqrt{\pi a}\, F\left(\theta, \frac{R}{t}\right) \tag{8}$$

The plastic functions h_1, h_2, and h_4 are also compiled.

The ABAQUS deformation theory routine utilizes a constitutive law which includes the elastic term (Eq. (1)), i.e., it is not a truly plastic solution. The analyses are performed to a load level in which plastic strains greatly dominate elastic strains everywhere in the body, which effectively results in a nearly fully plastic solution. However, for completeness, we obtain the fully plastic solution by subtracting out the (separately calculated) elastic results. Hence, from Eqs. (2) and (4), h_1, h_2, and h_4 are evaluated using[2]

[2]Note that Kumar et al. (1984) also compile f_3 and h_3, which are the axial stretch due to the crack. However, for bending (only) load, this displacement is not relevant.

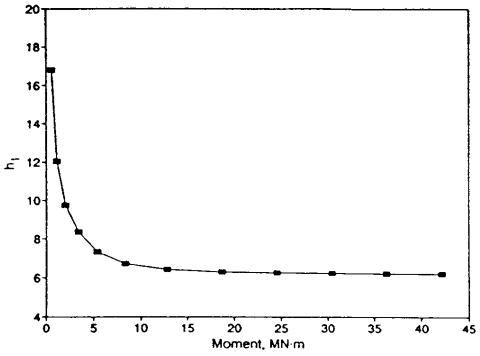

Fig. 2 Plasticity function h_1 (ABAQUS—solid element results) for pipe under bending, $R/t = 10$, $n = 3$, and $\theta/\pi = 0.0625$

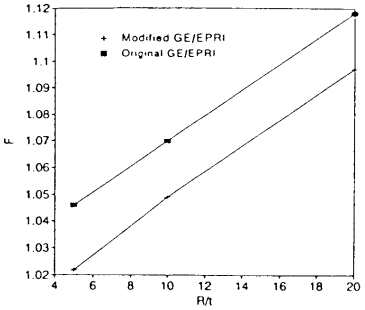

Fig. 3(a) F-function comparison

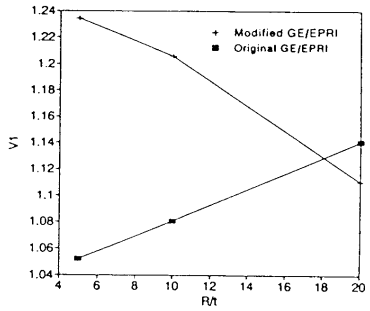

Fig. 3(b) V_1-function comparison

$$h_1 = \frac{J - J_e}{\alpha\sigma_o\epsilon_o a\left(1 - \frac{\theta}{\pi}\right)\left(\frac{M}{M_o}\right)^{n+1}} \tag{9}$$

$$h_2 = \frac{\delta - \delta_e}{\alpha\epsilon_o a\left(\frac{M}{M_o}\right)^{n}} \tag{10}$$

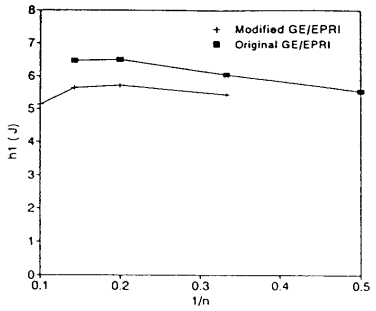

Fig. 4(*a*) Comparison of h_1-function, $R/t = 5$

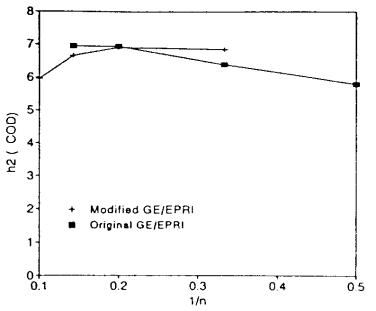

Fig. 5(*a*) Comparison of h_2-function, $R/t = 5$

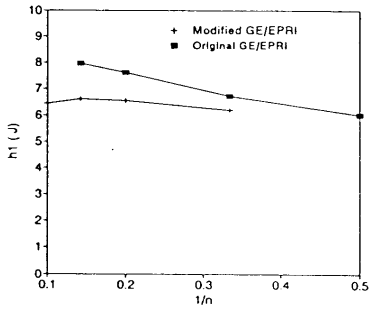

Fig. 4(*b*) Comparison of h_1-function, $R/t = 10$

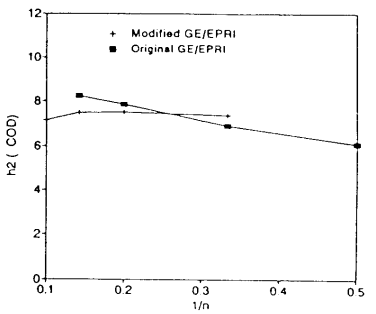

Fig. 5(*b*) Comparison of h_2-function, $R/t = 10$

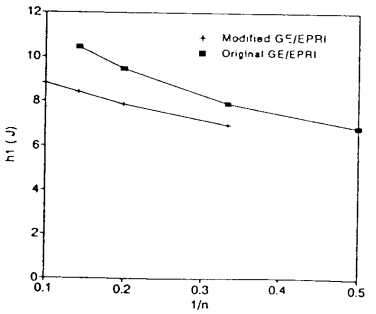

Fig. 4(*c*) Comparison of h_1-function, $R/t = 20$

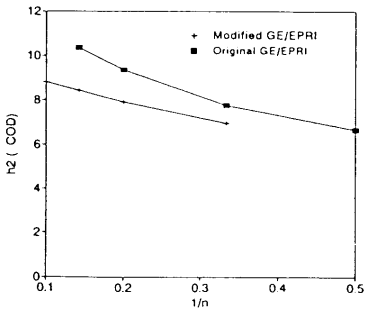

Fig. 5(*c*) Comparison of h_2-function, $R/t = 20$

$$h_4 = \frac{(\phi - \phi_e^c - \phi_e^{nc} - \phi_p^{nc})}{\alpha\epsilon_o \left(\frac{M}{M_o}\right)^n} \tag{11}$$

In Eqs. (9) to (11), respectively, J, δ, and ϕ are results from the ABAQUS solution. Also, in Eq. (11) the *nc* superscript refers to "no crack." These are well known and are listed in Kumar et al. (1984). The dimensionless elastic functions are compiled first (F, V_1, V_3) to determine J_e, δ_e, ϕ_c^e. Then the results of the ABAQUS solution provide J, δ, and ϕ, which are total values. Equations (9) to (11) provide h_1, h_2, h_4.

Results

It has been stated earlier that the GE/EPRI solutions appear to be inaccurate for small crack sizes. This may have been caused by the use of shell elements to compile the solutions, which may have led to overly stiff results. These errors are most vividly dramatized by observing that the pipe rotations due to the crack for small crack sizes, as compiled in Kumar et al. (1984), are negative for both elastic and plastic cases. This is physically impossible.

Table 1 shows the matrix of finite element calculations that were performed. A complete set of analyses was performed using ABAQUS on Battelle's Vax Computer for Model 2 ($n = 1$, 3, 5, 7, 10). Both elastic and fully plastic (deformation theory) computations were made for bending loads.

The GE/EPRI compilations appear to be more accurate for the large crack sizes. Hence, a comparison for the case of $R/$

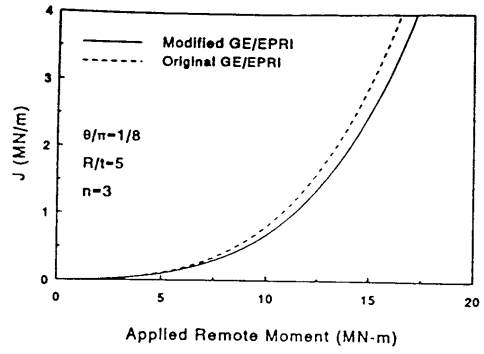

(a) n = 3

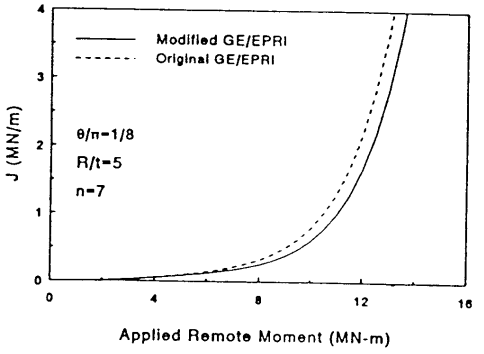

(b) n = 7

Fig. 6 Comparison of J versus moment for $R/t = 5$, $\theta/\pi = 1/8$

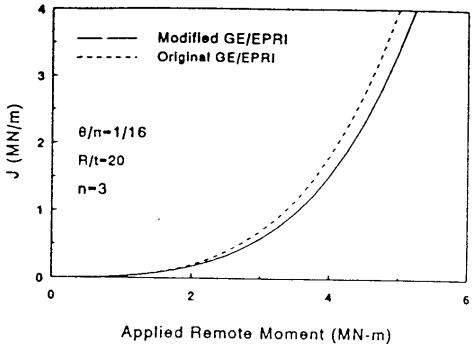

(a) n = 3

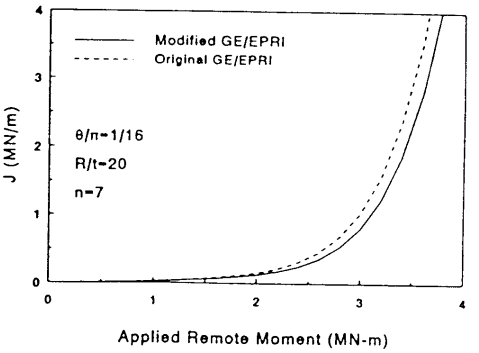

(b) n = 7

Fig. 7 Comparison of J versus moment for $R/t = 20$, $\theta/\pi = 1/16$

$t = 10$ was made to verify the accuracy of the approach taken here. For this case, $\theta/\pi = 0.5$ and $n = 3$ was chosen. Table 2 lists results. The comparison for the value of the J-integral (h_1) is very good. Further verification may be found in Wilkowski et al. (1992).

Tables 3 through 6 provide the solutions compiled for all of the cases listed in Table 1. Table 3 is the elastic solution, while Tables 4 to 6 provide solutions for $R/t = 5$, 10, and 20, respectively. Note that GE/EPRI did not provide solutions for $n = 10$ and some of the $n = 7$ cases due to numerical difficulties.

In order to obtain the h-functions, the ABAQUS calculation involved elastic and plastic analysis (deformation theory) for a series of bending moment loads until a fully plastic criteria was met. One check on the fully plastic h-functions reported in Tables 4 through 6 was to calculate these functions at all load levels and verify that h-functions do not vary once certain load levels (plasticity dominates) are reached. A typical plot of the h_1 function with bending moment is shown in Fig. 2 and it shows that the h_1 function levels off after some load value. This same technique was used to produce all of the h-functions.

Discussion

The differences between the previously developed solutions (Kumar et al., 1984) and the present results appear to be most important only for small crack sizes ($\theta/\pi = 1/8$, $1/16$). The present solutions were developing using the 3-dimensional solid elements (20-node brick) and the deformation theory algorithm of ABAQUS. The solutions presented here are believed to be the more accurate of the two solutions because full three-dimensional elements were used instead of relying on shell elements. However, the results of Kumar et al. (1984) are conservative. The analyses presented in Kumar et al. (1984) appeared to produce results that are too stiff, and, indeed, solutions for large n were not possible as convergence problems occurred. Here, no convergence problems were experienced. The problems with the small crack solutions of Kumar et al. (1984) are discussed in much more detail in Gilles and Brust (1991), Gilles et al. (1991), Brust and Gilles (1994), and Brust (1987).

A plot of the presently produced F-function results (Eq. (8)) and the GE/EPRI solution is seen in Fig. 3(a) as a function of R/t for $\theta/\pi = a/b = 1/16$, where a is the crack length and b is the uncracked ligament. The differences are about 3 percent. Figure 3(b) shows comparison of V_1 (Eq. (6)), which is related to the crack opening displacement. The differences are about 20 percent for $R/t = 5$. Comparison of h_1 (J-integral) and h_2 (crack opening displacement) are presented in Figs. 4 and 5, respectively. In these figures, note that the present solutions were not compiled for $n = 2$ ($1/n = 0.5$), while the GE/EPRI solutions were not compiled for $n = 10$ ($1/n = 0.1$). The h_1 and h_2 values differ by as much as 25 percent between the two solutions.

Finally, a comparison of J as a function of moment is made in Figs. 6, for $\theta/\pi = 1/8$, $R/t = 5$, and $n = 3$, 7; and, also Fig.

7 for $\theta/\pi = 1/16$, $R/t = 20$, and $n = 3$, 7. It is seen that the differences between the original and modified solutions can be significant.

No comparisons are made with the h_4 functions. As discussed earlier, the GE/EPRI h_4 functions are less than zero for most cases.

Conclusion

Solutions for the small circumferential crack under elastic-plastic conditions have been compiled for the case of pure bending. These are compiled in a format identical to that of Kumar et al. (1984). Solutions for the tension case and combined tension-bending are currently being compiled. Work is also continuing on the development of alternative improved estimation schemes for small cracks in pipe (Gilles and Brust, 1991) and a crack in a pipe weld (Rahman et al., 1991).

Acknowledgment

The authors would like to thank the Nuclear Regulatory Commission for financial support for this work.

References

Brust, F. W., 1987, "Approximate Methods for Fracture Analysis of Through-Wall Cracked Pipes," NUREG/CR-4853, Feb.

Brust, F. W., and Gilles, P., 1994, "An Equivalence Method for Estimating Energy Release Rates With Application to Cracked Cylinders".

Gilles, P., and Brust, F. W., 1991, "Approximate Methods for Fracture Analyses of Through-Wall Cracked Pipes, Part I, Theory," *Nuclear Engineering and Design*, Vol. 127, pp. 1-17.

Gilles, P., Chao, K. S., and Brust, F. W., 1991, "Approximate Methods for Fracture Analyses of Through-Wall Cracked Pipes, Part II, Applications," *Nuclear Engineering and Design*, Vol. 127, pp. 19-31.

Kumar, V., et al., 1984, "Advances in Elastic-Plastic Fracture Analysis," EPRI Final Report NP-3607, Aug.

Kumar, V., et al., 1981, "An Engineering Approach for Elastic-Plastic Fracture Analysis," EPRI Report NP-1931, July.

Rahman, S., Brust, F. W., Nakagaki, M., and Gilles, P., 1991, "An Approximate Method for Estimating Energy Release Rates of Through-Wall Cracked Pipe Weldments," *Proceedings of the 1991 ASME Pressure Vessel and Piping Conference*, San Diego, CA, June.

Rahman, S., and Brust, F. W., 1992, "An Estimation Method for Evaluating Energy Release Rates of Circumferential Through-Wall Cracked Pipe Welds," *Engineering Fracture Mechanics*, Vol. 43, No. 3, pp. 417-430.

Wilkowski, G. M., et al., 1992, "Short Cracks in Piping and Piping Welds," NUREG/CR-4599, BMI-2173, Vol. 1, No. 2, prepared by Battelle Memorial Institute.